Transport and Communications Science Journal

AN INTELLIGENCE-BASED OPTIMIZATION OF THE INTERNAL BURNISHING OPERATION FOR SURFACE ROUGHNESS AND VICKER HARDNESS

Can Xuan Khanh[1], Le Xuan Ba[2], Nguyen Truong An[1], Trinh Quang Hung[1], Nguyen Trung Thanh[1*]

[1]Department of Manufacturing Technology, Le Quy Don Technical University, No 236 Hoang Quoc Viet Street, Ha Noi, Vietnam

[2]CoBarny Limited Mechanical 25, Phu Minh Commune, Soc Son District, Ha Noi, Vietnam

*Corresponding author
Email: trungthanhk21@mta.edu.vn; trungthanhnguyen@lqdtu.edu.vn; Tel: 0982649266

Abstract. Boosting machining quality is a prominent solution to save production costs for burnishing operations. In this work, a machining condition-based optimization has been performed to decrease surface roughness (SR) and enhance Vickers hardness (VH) of the minimum quantity lubrication-assisted burnishing operation (MQLABO). The burnishing factors are the spindle speed (S), depth of penetration (D), and the air pressure (P). The burnishing trails of the hardened material labeled 40X have been conducted on a milling machine. The adaptive neuro-based-fuzzy inference system (ANFIS) was used to construct the correlations between the process inputs and MQLABO responses. The non-dominated sorting genetic algorithm-II (NSGA-II) is utilized to determine the optimal parameters. The scientific outcomes revealed that the optimal values of the S, D, and P are 800 RPM, 0.09 mm, and 4.0 Bar, respectively. The SR is decreased by 53.8%, while the VH is enhanced by 3.1%, respectively, as coBarred to the initial values.

Keywords: Internal burnishing, Surface roughness, Vickers hardness, Minimum quantity lubrication, Optimization.

1. INTRODUCTION

The burnishing technology, one of the finishing machining methods using the surface plastic deformation has been widely applied to produce various mechanical components. The

profile irregularities generated by the former operation will be compressed under the influences of the burnishing pressure. Some benefits obtained include a low roughness, high surface hardness, deeper thickness of the hardened layer, and compressive stress. Moreover, the component's functionality has been greatly improved, contributing significantly to increasing strength behaviour and abrasion as well as chemical corrosion resistances. The burnishing process has great potential to replace traditional approaches, such as grinding, honing, lapping, and polishing.

The optimal factors of different burnishing operations have been selected for improving machining responses. The response surface method (RSM) was utilized to obtain optimal parameters for the ball burnishing process of T215Cr12 material [1]. The parameters were the burnishing speed (V), feed rate (f), burnishing pressure (P), and the number of passes (NP), while the objectives included the surface roughness (SR) and surface hardness (SH). The outcomes indicated that the optimal values of the SR and SH were 0.055 μm and 46.69 HRC, respectively. The optimal values of the f, NP, burnishing force (F), step-over (SO), and the ball diameter (db) were obtained to improve the SR and SH of the burnished Al 63400 [2]. The results showed that the optimum values of the SR and SH were 0.032 μm and 91.63 HV, respectively. Cobanoglu and Ozturk explored the effects of the V, f, and F on the SR and SH of the burnished AISI 1040 steel [3]. The results presented that the SR and SH were enhanced by 100.0% and 55.50%, as coBarred to the initial values. Banh and Shiou revealed that the SR and SH of the burnished STAVAX material were improved by 91.0% and 8.0%, respectively at the optimal solution with the aid of the burnishing operation [4]. The empirical models of the SR and SH for the burnished TA2 alloy were proposed in terms of the V, f, and the depth of penetration (D) [5]. The authors stated that the enhancements in the SR and SH were 63.0% and 28.0%, respectively.

The RSM models of the SR, SH, and profile irregularities (PI) were developed in terms of the V, f, and D [6]. The results exhibited that the enhancements of the SR, PI, and HA were 81.0%, 34.0%, and 17.0% at the optimal solution. The changes in the residual stress (RS), roundness (RO), SR, and SH under the iBarct of the ultrasonic burnishing for 34CrNiMo6-M steel were explored [7]. The results indicated that the RS and SR could be improved by 90.0% and 400.0%, while the RO was enhanced by 38.0%. The regression models of the SR and SH for the ultrasonic-assisted burnishing process of the aluminium alloy were developed by Teimouri et al. [8]. The authors concluded that the proposed approach could bring a higher value of the affected depth. An analytical model has been developed to forecast the burnishing force in the processing time [9]. The factors, including the f, D, db, and the number of rollers (N) were taken into account the model. The small errors indicated that the model proposed could be used to forecast technical performance. The regression models of the SR, SH, and the depth of affected layer (AL) were developed regarding the V, f, and D for the internal burnishing operation of carbon steel [10]. The authors stated that a set of feasible solutions could be employed to enhance surface properties. Moreover, Nguyen and Le revealed that the SR and SH could be improved by 96.0% and 45%, respectively [11]. The iBarcts of the V, f, and D on the energy consumption (EC), power factor (PF), SR, and SH for the flat burnishing operation of the die steel were explored by Nguyen et al. [12]. The improvements of the EC, SR, SH, and the PF were 49.5%, 13.8%, 21.8%, and 56.0%, respectively. The Kriging models of the EC, SH, and mean roughness square (Rz) for the burnishing process were developed by Nguyen et al. [13]. The findings indicated that the EC and R_z were decreased by 39.5% and 7.8%, respectively, while the SH was increased by 29.6%.

As a result, different burnishing processes have been optimized to improve the machining performances, such as the surface roughness, surface hardness, residual stress, energy consumption, the depth of the affected layer, and power factor. The common inputs are the burnishing speed, feed, force, pressure, step-over, and the number of passes. Besides, various optimization approaches, such as Taguchi and RSM have been employed to render the correlations and obtain optimal values. Unfortunately, the deficiencies of published works for different burnishing processes can be listed as follows:

The technical performances of different burnishing operations under the flooding lubrication have been extensively explored. However, the influences of machining parameters on the machining quality for the internal burnishing operation under the minimum quantity lubrication (MQL) environment have not been analysed.

The comprehensive models of the surface roughness and hardness in terms of process parameters for the internal burnishing process under the MQL condition have not been developed. It is necessary to develop a predictive model under a variety of machining parameters, which can be used for prediction purposes.

To bridge these analysed research gaps, an effective optimization of the minimum quantity lubrication-assisted burnishing operation (MQLABO) has been addressed to decrease the surface roughness (SR) and enhance the Vickers hardness (VH). The industrial steel labelled 40X is extensively employed to produce military components having deep holes and high-pressure bushings. The predictive models of the machining responses are proposed using the adaptive neuro-based fuzzy inference system and experimental data. The optimal factors are determined with the support of the non-dominated sorting genetic algorithm-II (NSGA-II).

2. OPTIMIZATION FRAMEWORK

2.1. Optimization issues

In this investigation, two quality responses, including the surface roughness and the Vickers hardness are optimized to enhance the surface properties.

The surface roughness SR (µm) is calculated as:

$$SR = \frac{\sum_{i=1}^{5} R_{ai}}{5} \tag{1}$$

where, R_{ai} presents the arithmetic roughness after the burnishing operation at the measured position.

The Vickers hardness VH (HV) is calculated as:

$$VH = \frac{\sum_{i=1}^{5} VH_{ai}}{5} \tag{2}$$

where, VH_{ai} denotes the Vickers hardness after the burnishing operation at the measured position.

Table 1. MQLABO parameters for the optimization process.

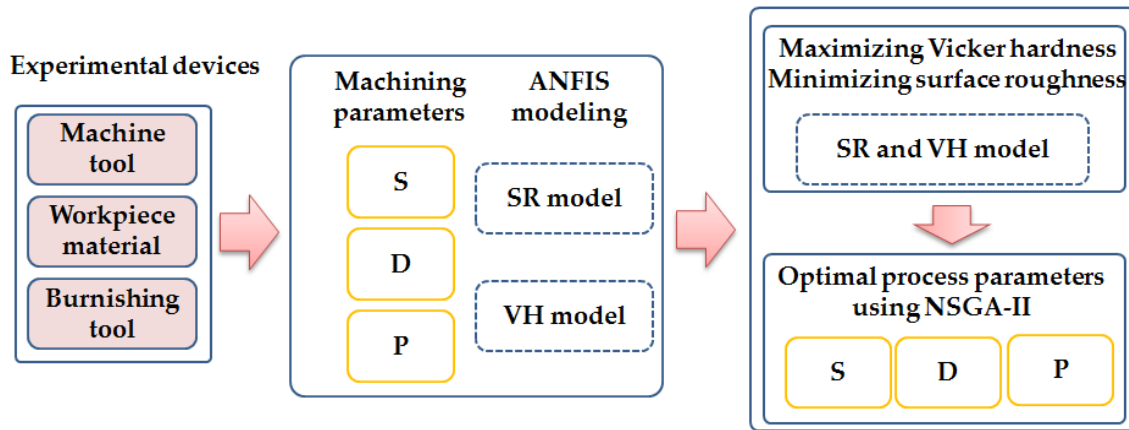| Symbol	Parameters	Level 1	Level 2	Level 3
S	Spindle speed (RPM)	560	800	1120
D	Burnishing depth (mm)	0.06	0.08	0.10
P	Air pressure (Bar)	2	3	4

Figure 1. Optimization approach for the MQLABO.

For the MQLABO, affecting factors are process parameters (speed, burnishing feed, burnishing depth), the characteristics of lubrication (air pressure, oil flow rate, kinds of the fluid, number of nozzles), the configuration of burnishing tool (number of rollers, roller material, and roller dimensions). In this work, the spindle speed, burnishing depth, and air pressure are listed as machining factors, as shown in Table 1.

The ranges of the spindle speed are selected based on recommend values associated with the machine tool. The levels also are tested with the recommendations of the manufacturers for the burnishing tool. The lowest and highest levels of the burnishing depth are determined based on the dimension of the pre-machined hole and the properties of the workpiece. Moreover, these ranges are verified with the advice of the manufacturers for the burnishing tool to prevent the deterioration of rollers. The pressure values are selected using the recommended ranges associated with the minimum quantity lubrication (MQL) device. These ranges are tested using the burnishing experiments at the lowest and highest levels to ensure the machinability.

The optimization issue can be expressed as:

Find X = [S, D, and P]

Minimize SR and maximize VH.

Constraints: $560 \leq S \leq 1120$ (RPM); $0.06 \leq D \leq 0.10$ (mm); $2 \leq P \leq 4$ (Bar).

2.2. Optimization approach

The optimization approach for the MQLABO to generate optimal factors is expressed as follows (Fig. 1):

Step 1: The internal burnishing experiments using parameter combinations are performed to obtain the data.

Step 2: The ANFIS approach is employed to develop the predictive models of the SR and VH in terms of machining parameters [14, 15].

In this research, the ANFIS approach is used instead of traditional approaches (RSM and regression method) to describe the iBarcts of input process parameters on the surface roughness and Vickers hardness. ANFIS has been considered as an intelligent approach, which takes the best advantages of the artificial neural network (ANN) and fuzzy interface system (FIS). The ANFIS is named as a power full method to describe the highly non-linear data when the experimental results are complex. ANFIS has a huge number of parameters and can adapt very well to limited amounts of data. This approach has various advantages,

including the rapid learning capacity, the seizing nonlinear structure of a process, adaptive capability, and is not requiring expert knowledge. The ANFIS model is trained and learned without relying solely on expert knowledge to propose the fuzzy logic model. The ANFIS correlation is more transparent to the user and causes less memorization errors, as coBarred to the ANN. Consequently, the ANFIS is widely implemented to solve engineering issues.
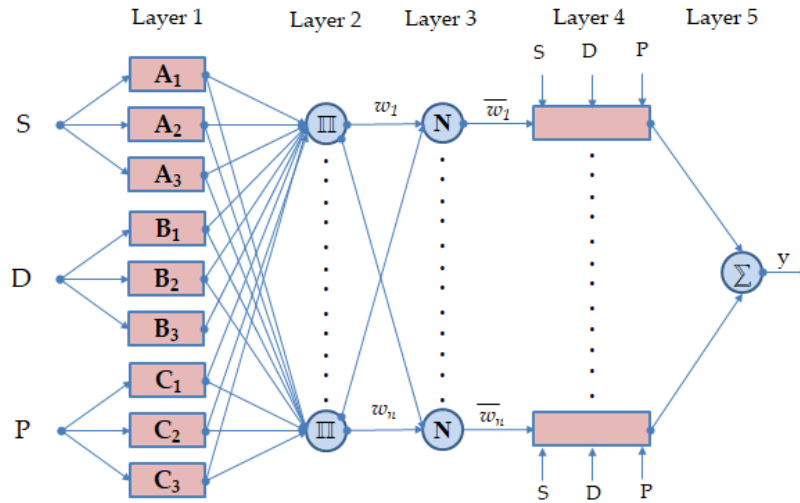

Figure 2. The typical structure of the ANFIS model.

The fuzzy rules and learning algorithms of the ANN are employed to present the uncertain and nonlinear process control system. The operating parameters of the ANFIS model are the number and types of input membership functions (triangular, trapezoidal, bell-shaped, Gaussian, and sigmoid), type of output membership functions (constant or linear), optimization methods (hybrid or back-propagation), and the number of epochs. It is necessary to select the optimal combination of the mentioned parameters for increasing the reliability and accuracy of the network. The primary rule of the ANFIS is expressed as:

$$Rule\ 1 : If\ x_1\ is\ A_1\ and\ x_2\ is\ B_1,\ then\ y_1 = a_1x + b_1x + c_1 \tag{3}$$
$$Rule\ 2 : If\ x_2\ is\ A_2\ and\ x_2\ is\ B_2,\ then\ y_1 = a_2x + b_2x + c_2 \tag{4}$$

where x and y are input and output. A_i and B_i denote the membership functions of each of the input x_1 and x_2, respectively. a_i, b_i and c_i are constants.

The designed ANFIS model using five-layer feed forward neural networks for the MQLABO responses is expressed as follows (Fig. 2):

Layer 1 (Fuzzification layer): The primary duty of the first layer is to select the membership degrees for each input using the given membership functions (MF). The outputs of this layer are identified as:

$$L_1^i = M_1^i = \mu_{A_i}(x) \tag{5}$$

where x is the input of the i_{th} node. A_i presents the linguistic variable associated with this node function and μ_{Ai} denotes the membership function of A_i.

Layer 2 (Rule layer): This layer comprises circle nodes namely Π. The primary duty of the second layer is to collect the inputs from the respective fuzzification nodes and determine the firing strength ω_i of the rule. The output presenting the firing strength is presented as:

$$L_2^i = \omega_i = \mu_{A_i}(x) \times \mu_{A_i}(y), i = 1, 2, 3...N \tag{6}$$

Layer 3 (Normalized layer): This layer comprises fixed nodes namely N. The primary duty of the third layer is to evaluate the ratio of the firing strength of a given rule to the total of firing strengths of all rules. The output presenting the normalized firing strength is represented as:

$$L_3^i = \bar{\omega}_i = \frac{\omega_i}{\sum_{i=1}^{n} \omega_i}, i = 1, 2, 3..., N \tag{7}$$

Layer 4 (Defuzzification layer): This layer comprises squared nodes. The primary duty of the forth layer is to defuzzificate received inputs and assign the consequent parameters of the rules. The output of this layer is expressed as:

$$L_{4,i} = \bar{\omega}_i y_i = \bar{\omega}_i(a_i x + b_i x + c_i), i = 1, 2, 3, ..., N \tag{8}$$

where a_i, b_i, and c_i are the consequent parameters, respectively.

Layer 5 (Output layer): This layer comprises a fixed node. The primary duty of the fifth layer is to calculate the overall output as the summation of all incoming signals. The output of this layer is expressed as:

$$L_{5,i} = \sum_i \bar{\omega}_i f_i = \frac{\sum_i \omega_i f_i}{\sum_i \omega_i} \tag{9}$$

Step 3: Determination of the optimal factors using non-dominated sorting genetic algorithm-II (NSGA-II).

NSGA-II is a powerful optimization technique to solve the trade-off analysis between the conflicting responses. This algorithm brings a non-dominated sorting approach, which is effectively applied to select the global optimization results. The operating procedure of the NSGA-II is shown in Fig. 3 and referenced in the work of [16].
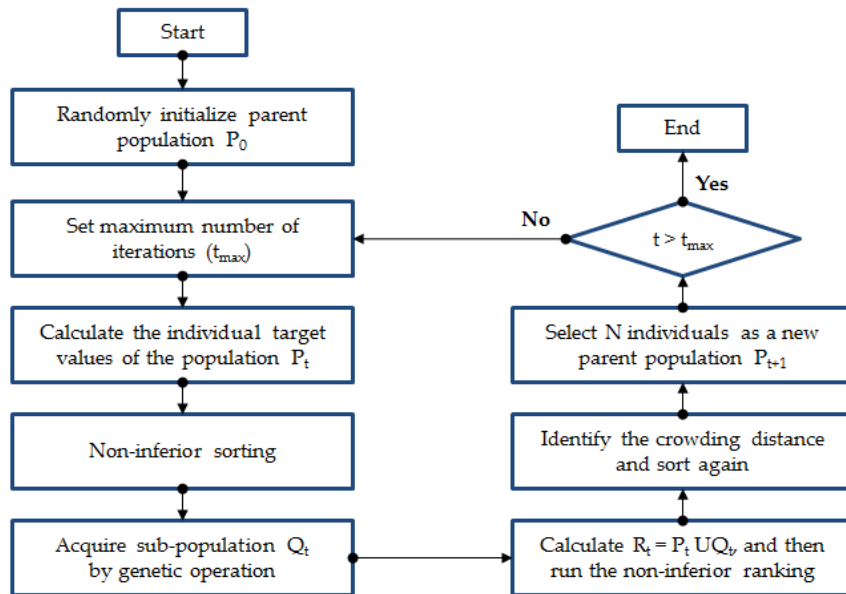

Figure 3. Operating principle of the NSGA-II.

3. EXPERIMENTS AND MEASUREMENTS

The burnishing samples are made of the hardened steel labelled 40X steel. The pre-machining processes, including the drilling and turning are applied to produce the through-hole in each specimen. The dimensions are the length of 42 mm, the internal diameter of 28 mm, and the outer diameter of 38 mm, respectively. The average roughness and Vickers hardness of the machined surface are approximately 3.09 µm and 500.8 HV, respectively.

The burnishing trails are done with the aid of a milling machine namely GS-300A (Fig. 4). The spindle speed ranges from 90 RPM to 3800 RPM. The feed rate of 0.07 mm/rev. is employed for all experiments. The spindle speed values are selected based on the assigned ranges in the milling machine.

The workpiece is positioned and tightly clamped using the three-jaw self-centering chuck. The chuck used is then tightly fixed with the aid of the precision vise. The burnishing tool is clamped on the machine spindle using the straight shank. The linear motion of the burnishing tool is conducted with the support of the Z-axis. The burnishing depth is defined as the perpendicular distance between the original and adjusted diameters of the burnishing tool. After adjustment of the assigned diameter, the burnishing tool is employed to execute the burnishing trails.

The minimum quantity lubrication (MQL) system is used in conjunction with the soybean oil to supply the lubricant into the burnishing region. The minute amount of the soybean oil is mixed with the compressed air to form an air-oil mist. The pressure regulator and flow meter are used to control and regulate the compressed air and flow rate. The values of the air pressure are adjusted using the regulator based on recommended ranges of the MQL system, as shown in the gauge. After adjustment, the air pressure is kept at the assigned value to perform the experiment.
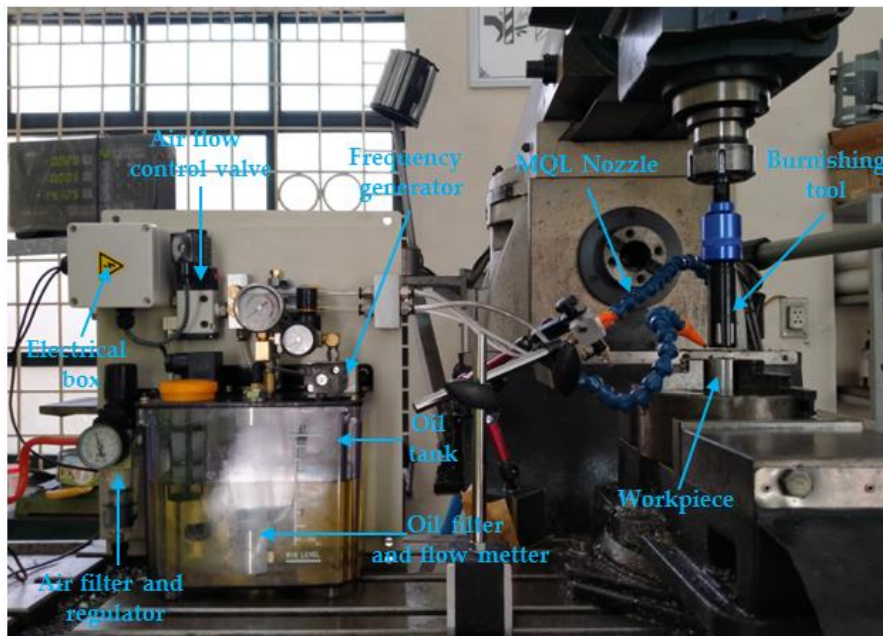

Figure 4. Experimental setting.

(a) Measuring roughness   (b) Measuring Vickers hardness
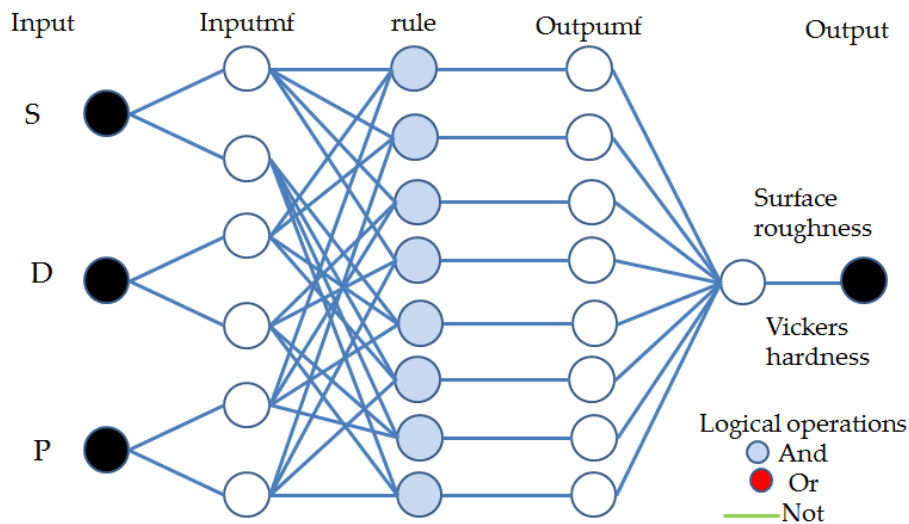
Figure 5. Measuring responses.

Figure 6. The 2-2-2-2 structure of ANFIS model for the MQLABO response.

The roughness is measured in three different points of the burnished surface according to the ISO 4287 using a tester namely Mitutoyo Surftest-301 (Fig. 5a). The measured length of 4.0 mm is employed for all machining specimens. The measured range of 0.05-40 mm and the resolution of 0.01 mm are employed to enhance accuracy.

The Vickers hardness is measured in three different points on the burnished surface using a tester namely Wilson Wolpert (Fig. 5b). The pressed load of 29.42 N and the dwell time of 10 seconds are used for each hardness testing. The measured specimen having dimensions of 10 x 10 mm^2 is produced using the Wire electrical discharge machining process.

4. RESULTS AND DISCUSSIONS

4.1. Development of ANFIS models

The experimental outcomes of the MQLABO are shown in Table 2, in which the obtained data from 1 to 27 are employed to develop ANFIS models.

The 2-2-2-2 structure of the ANFIS model is employed to present the relation between MQLABO parameters and the SR as well as VH models (Fig. 6). The membership function labelled *gaussmf* is applied to obtain minimal deviations (Table 3).

The operating parameters, including the type of output membership functions, optimization methods, and the number of epochs for the proposed ANFIS models are shown in Table 4.

4.2. ANOVA results

ANOVA analysis is applied to find the significant parameters and model adequacy. The ANOVA results of the SR and VH model are shown in Table 5 and 6, respectively. The R^2-values of the SR and VH models are 0.9883 and 0.9850, respectively, which revealed that the developed ANFIS models are significant. The factors having p-value less than 0.05 are significant. For the SR model, the single terms (S, D, and P), the interactive term (DP), and the quadratic terms (S^2 and D^2) are named as the significant factors.

For the VH model, the single terms (S, D, and P), the interactive term (SD and DP), and the quadratic terms (S^2, D^2, and P^2) are named as the significant factors.

Table 2. Experimental data for the MQLABO.

No.	S (RPM)	D (mm)	P (Bar)	SR (µm)	VH (HV)
1	560	0.06	2.0	0.66	533.7
2	560	0.08	2.0	0.43	554.3
3	560	0.10	2.0	0.33	554.8
4	560	0.06	3.0	0.52	552.3
5	560	0.08	3.0	0.31	571.9
6	560	0.10	3.0	0.22	571.5
7	560	0.06	4.0	0.41	565.3
8	560	0.08	4.0	0.23	584.1
9	560	0.10	4.0	0.15	582.8
10	800	0.06	2.0	0.61	560.8
11	800	0.08	2.0	0.38	582.1
12	800	0.10	2.0	0.28	583.3
13	800	0.06	3.0	0.47	579.4
14	800	0.08	3.0	0.26	599.8
15	800	0.10	3.0	0.18	600.1
16	800	0.06	4.0	0.36	592.5
17	800	0.08	4.0	0.17	612.2
18	800	0.10	4.0	0.11	611.4
19	1120	0.06	2.0	0.59	554.6
20	1120	0.08	2.0	0.37	576.9
21	1120	0.10	2.0	0.28	579.4
22	1120	0.06	3.0	0.47	573.3
23	1120	0.08	3.0	0.26	594.7
24	1120	0.10	3.0	0.18	595.9
25	1120	0.06	4.0	0.35	586.5
26	1120	0.08	4.0	0.19	607.8
27	1120	0.10	4.0	0.12	607.4

Table 3. The errors for different ANFIS models.

| ANFIS models	Membership functions		
	gbellmf	gaussmf	gauss2mf
For the surface roughness SR	0.00208	0.00154	0.00198
For the Vicker hardness VH	0.04937	0.04546	0.04798

Table 4. The parameters for different ANFIS models.

ANFIS models	Number of MFs	Types of output MFs	Optimal method	The number of epochs
For the surface roughness SR	2-2-2-2	Linear	Hybrid	100
For the Vicker hardness VH	2-2-2-2	Linear	Hybrid	100
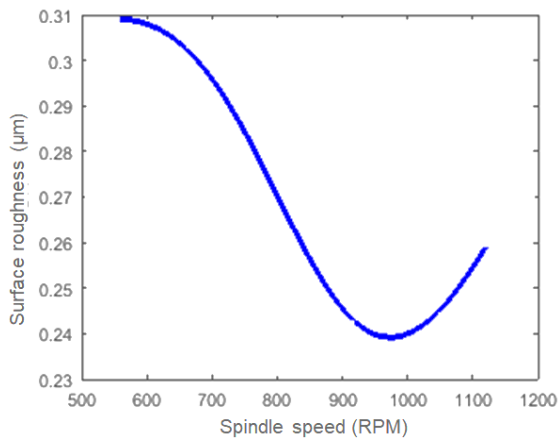
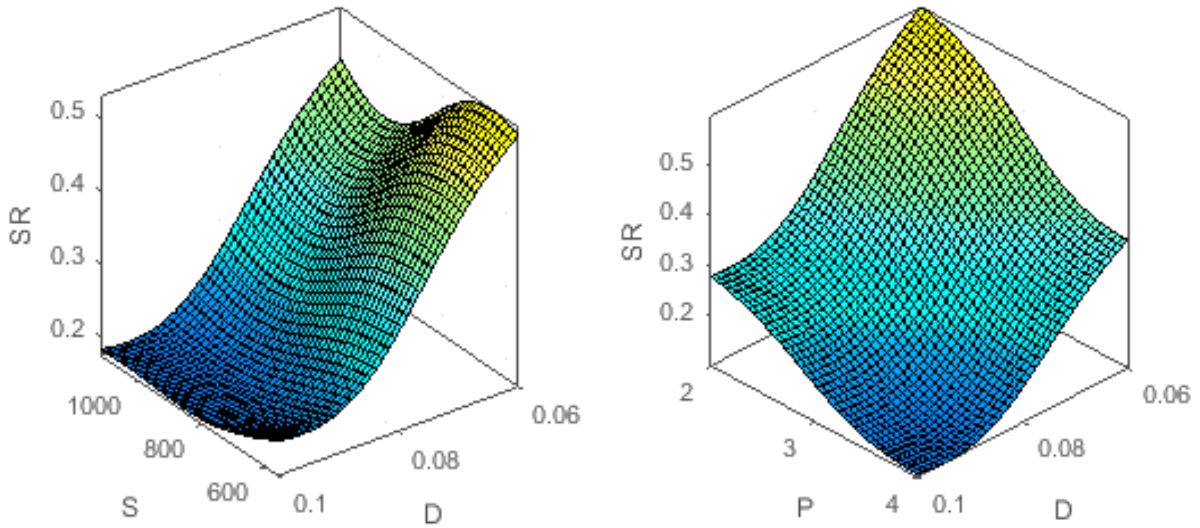(a) Surface roughness versus the spindle speed
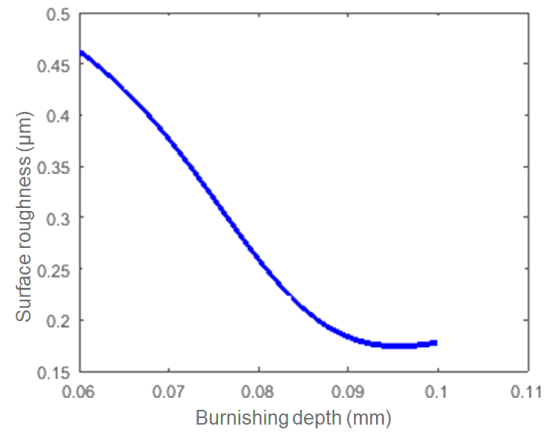
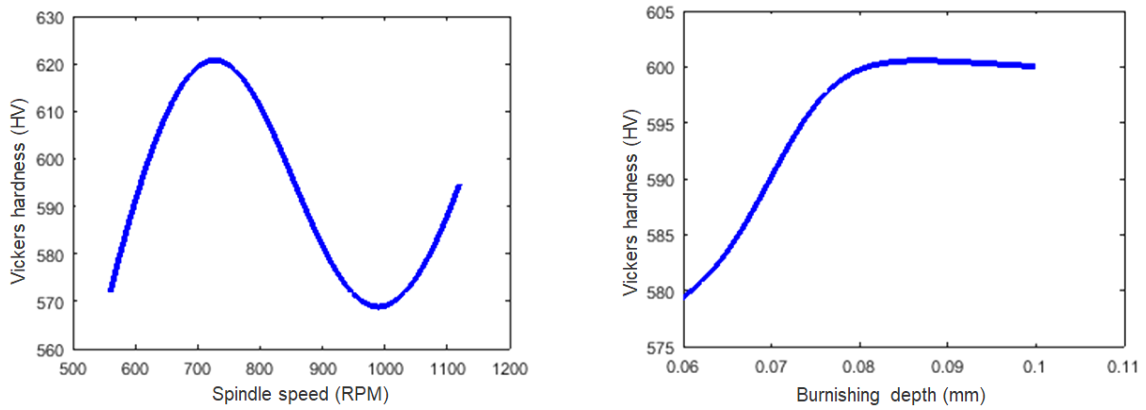(b) Surface roughness versus the burnishing depth
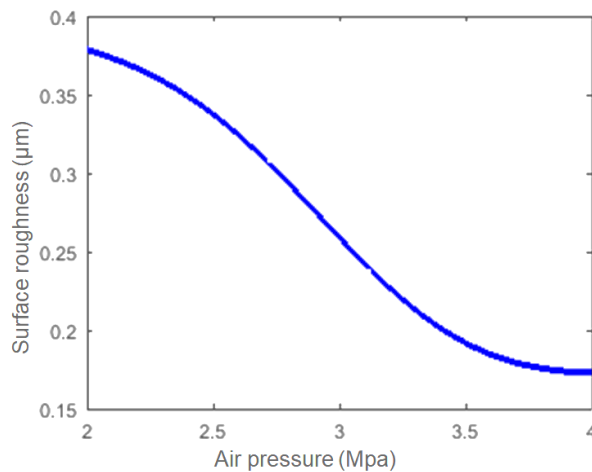
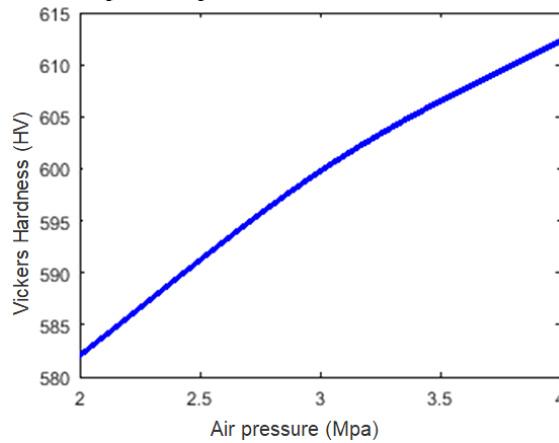(c) Surface roughness versus the air pressure

Figure 7. The main influences of the MQLABO parameters on the SR.

(a) Surface roughness versus the spindle speed and burnishing depth

(b) Surface roughness versus the burnishing depth and air pressure

Figure 8. The interactive influences of the MQLABO parameters on the SR.
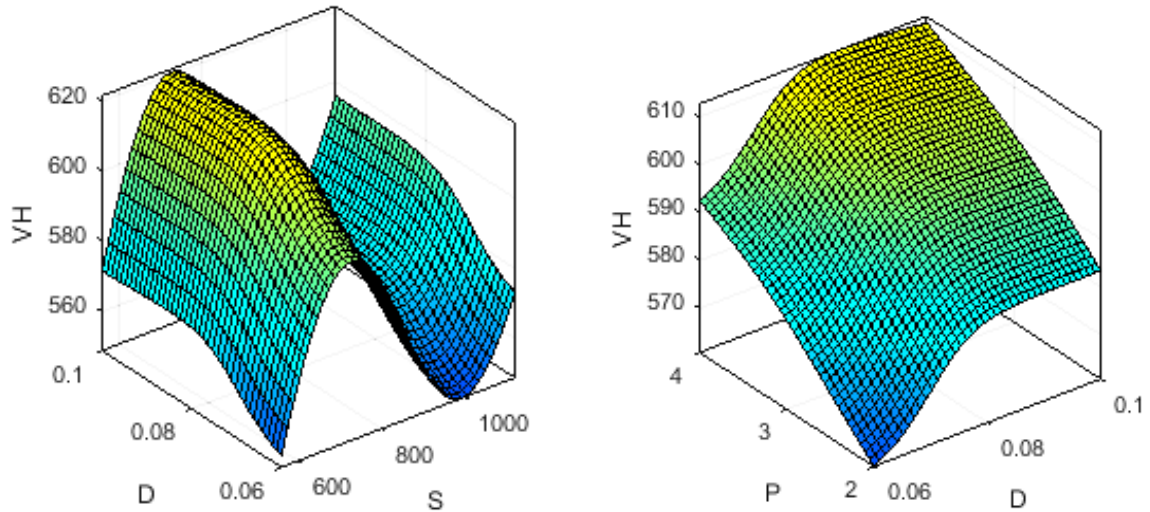

(a) Vickers hardness versus the spindle speed

(b) Vickers hardness versus the burnishing depth

(c) Vickers hardness versus the air pressure

Figure 9. The main influences of the MQLABO parameters on the VH.

(a) Vicker hardnesss versus the spindle speed and burnishing depth

(b) Vickers hardness versus the burnishing depth and air pressure

Figure 10. The interactive influences of the MQLABO parameters on the VH.

Table 5. ANOVA results for SR model.

Source	Sum of Squares	Mean Square	F Value	p-value	Remarks	Contribution (%)
Model	0.26539	0.02949	235.90	< 0.0001	Significant	
S	0.00500	0.00500	40.00	0.0032	Significant	1.87
D	0.16245	0.16245	1299.60	< 0.0001	Significant	60.72
P	0.08405	0.08405	672.40	< 0.0001	Significant	31.42
SD	0.00010	0.00010	0.80	0.4216	Insignificant	0.04
SP	0.00010	0.00010	0.80	0.4216	Insignificant	0.04
DP	0.00160	0.00160	12.80	0.0232	Significant	0.60
S^2	0.00200	0.00200	16.00	0.0161	Significant	0.75
D^2	0.01152	0.01152	92.16	0.0007	Significant	4.31
P^2	0.00072	0.00072	5.76	0.0744	Insignificant	0.27
Residual	0.00314	0.00013	2140.32			
Total	0.26853					
R^2	0.9883					

Table 6. ANOVA results for VH model.

Source	Sum of Squares	Mean Square	F Value	p-value	Remarks	Contribution (%)
Model	4956.576	550.731	1855.093	< 0.0001	Significant	
S	1032.851	1032.851	3479.078	< 0.0001	Significant	20.03
D	877.805	877.805	2956.817	< 0.0001	Significant	17.03
P	1797.001	1797.001	6053.057	< 0.0001	Significant	34.86
SD	2.890	2.890	9.735	0.0355	Insignificant	0.06
SP	0.023	0.023	0.076	0.7967	Insignificant	0.00
DP	3.240	3.240	10.914	0.0298	Significant	0.06

S^2	1093.721	1093.721	3684.111	< 0.0001	Significant	21.21
D^2	324.013	324.013	1091.411	< 0.0001	Significant	6.28
P^2	23.981	23.981	80.776	0.0008	Insignificant	0.47
Residual	75.481	0.297	17365.974			
Total	5032.057					
R^2	0.9850					

4.3. Parametric effects

Fig. 7 presents the main influences of the MQLABO parameters on the SR. Low surface roughness is desirable to enhance the machining quality.

Fig. 7a presents the iBarct of the S on the SR. As a result, the roughness is decreased with an increased S, while further speed results in a higher roughness. When the spindle speed increases, the temperature in the burnishing region increases; hence, the workpiece hardness and strength are decreased. The material is easily compressed and the roughness is significantly reduced. Further spindle speed may lead the excessive machining temperature, the work-hardening behavior may occur on the burnished surface. The machined surface is hardly burnished; hence a higher roughness is produced.

Fig. 7b presents the iBarct of the D on the SR. A low burnishing depth causes a reduction in the machining pressure and a small amount of material is compressed. A small degree of plastic deformation is produced, which causes a higher roughness. An increased burnishing depth leads to a higher machining pressure, which causes a larger degree of plastic deformation. A higher amount of the material is compressed and low roughness is produced.

Fig. 7c presents the iBarct of the P on the SR. It can be stated that lower roughness is obtained with an increase in the air pressure. The primary reason is that higher pressure causes a reduction in the droplet size of the oil mist. A small diameter increases the penetration ability into the burnishing region; hence, the lubrication effectiveness is enhanced. The friction between the burnishing tool and workpiece is decreases and the roughness value is reduced.

The interactive iBarcts of the MQLABO parameters on the SR are shown in Fig. 8.

Fig. 9 presents the main influences of MQLABO parameters on the VH. For the burnishing process, higher VH is preferred to enhance the machining quality.

Fig. 9a presents the iBarct of the S on the Vickers hardness. As a result, a higher VH value is found with an increment in the S. After maximizing point, further spindle speed leads to a decrement in the hardness. A higher spindle speed results in an increased machining temperature, which causes an improvement in the larger plastic deformation. The Vicker hardness is consequently enhanced with increased spindle speed. Unfortunately, a further speed may cause excessive burnishing temperature and the residual stress can be relieved; hence, the VH value is decreased.

Fig. 9b presents the iBarct of the D on the Vickers hardness. As a result, a higher VH value is found with an increment in the D. After maximizing point, further depth speed leads to a slight decrement in the hardness. An increased D causes a larger degree of work-hardening, resulting in a higher VH value. Unfortunately, a further depth may cause excessive burnishing temperature and the residual stress can be relieved; hence, the VH value is decreased.

Fig. 9c presents the iBarct of the P on the Vickers hardness. A higher VH value is produced with an increased P. An increased P leads to an increment in the lubrication effectiveness, which reduces the machining temperature. The diminishing of the residual stress is prevented; hence the Vickers hardness is enhanced.

The interactive iBarcts of the MQLABO parameters on the VH are shown in Fig. 10.

The images of the pre-machined and burnished surfaces are captured with the aid of a scanning electron microscope labeled Nano Nova 450 at the 2000 level of the magnification. The big holes and large cracks are generated by the rough drilling and turning operations, as shown in Fig. 11a. The machined defects are burnished with the support of the burnishing process; hence, a smooth surface is produced (Fig. 11b). It can be stated that the burnishing process has a significant contribution to a reduction in the surface roughness.
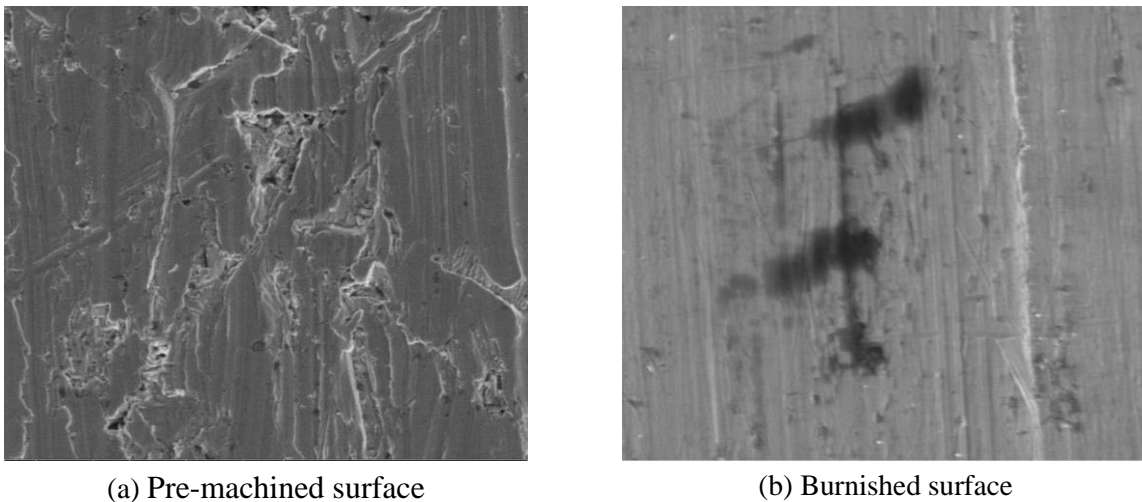

(a) Pre-machined surface   (b) Burnished surface

Figure 11. The images of the pre-machined and burnished surfaces.

4.4. Optimization results

The ANFIS models of the surface roughness and Vickers hardness are applied to select the optimal factors. The Pareto fronts generated by NSGA-II are shown in Fig. 12.

Based on the optimization requirement, the solution no. 268 is selected as the optimal point. As a result, the optimum values of the spindle speed, burnishing depth, and the air pressure are 800 RPM, 0.09 mm, and 4.0 Bar, respectively. The reduction in the surface roughness is 53.8% while the Vickers hardness is enhanced by 3.1%, as coBarred to the initial values (Table 7).

Table 7. Optimization results for the MQLABO.

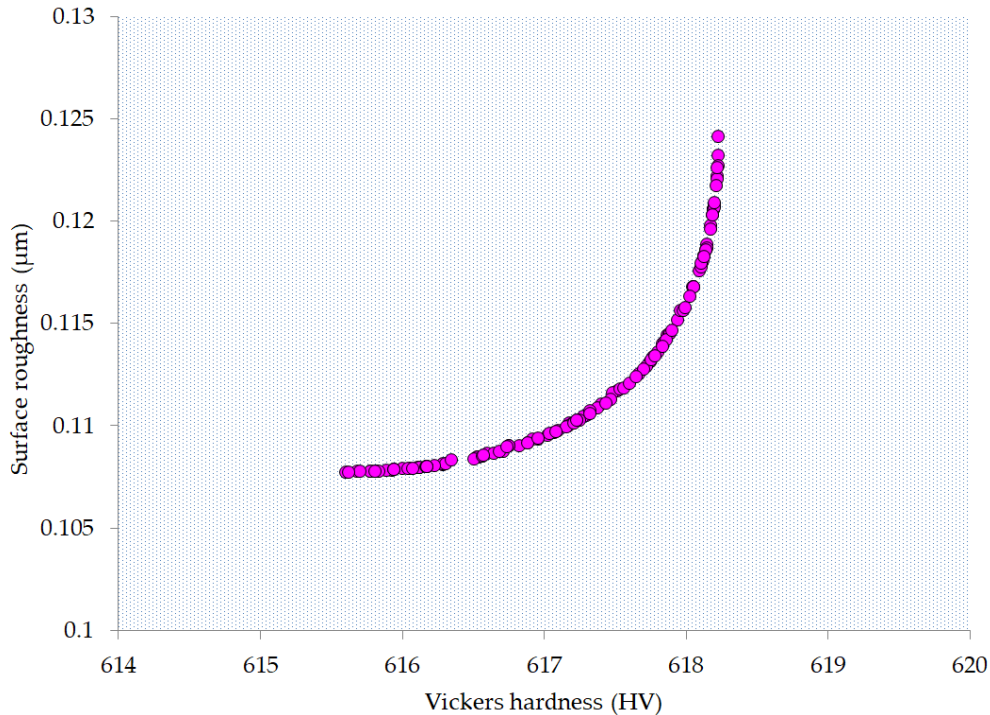| Method	Optimization parameters			Responses	
	S (RPM)	D (mm)	P (Bar)	SR (µm)	VH (HV)
Initial values	800	0.08	3.0	0.26	599.8
Optimal results	800	0.09	4.0	0.12	618.2
Improvement (%)				-53.8	3.1

Figure 12. Pareto graphs.

5. CONCLUSIONS

In the current work, an attempt has been made to optimize the machining conditions of the roller burnishing operation for reducing the surface roughness and improving the Vickers hardness under the minimum quantity lubrication. The inputs are the spindle speed, burnishing depth, and the air pressure. The ANFIS method was applied to develop comprehensive models of the burnishing responses regarding the process parameters. The NSGA-II was utilized to find optimal outcomes. The finding can be listed as bellows:

1. The highest values of the burnishing depth and the air pressure can be applied to decrease the surface roughness, while the middle level of the spindle speed is recommended to apply. The middle values of the spindle speed and burnishing depth are recommended to enhance the Vickers hardness, while the highest air pressure can be used.

2. The ANFIS models of the surface roughness and Vickers hardness are soundness and significance. Moreover, the proposed models can be directly employed for the roller burnishing operation of the hardened 40X steel without expensive experimental costs and efforts.

3. As shown in the optimal setting generated by NSGA-II, the optimal parameters of the S, D, and P are 800 RPM, 0.09 mm, and 4.0 Bar, respectively. The SR is decreased by 53.8%, while the VH is enhanced by 3.1%, respectively in coBarrisons with the initial values.

4. The proposed approach using the ANFIF and NSGA-II can be used to model the comprehensive responses and to effectively select the optimal solution, as coBarred to the trial method and operator experience.

ACKNOWLEDGMENT

REFERENCES

[1]. R. S. John, B. K.Vinayagam, Optimization of ball burnishing process on tool steel (T215Cr12) in cnc machining centre using response surface methodology, Arab. J. Sci. Eng., 36 (2011) 1407-1422. https://doi.org/10.1007/s13369-011-0126-9

[2]. M. R. S. John, B. K. Vinayagam, Optimization of nonlinear characteristics of ball burnishing process using Sugeno fuzzy neural system, J. Braz. Soc. Mech. Sci. & Eng., 36 (2014) 101-109. https://doi.org/10.1007/s40430-013-0060-8

[3]. T. Cobanoglu, S. Ozturk, Effect of burnishing parameters on the surface quality and hardness, P. I. Mech. Eng. B-J. Eng., 229 (2015) 286-294. https://doi.org/10.1177/0954405414527962

[4]. Q. N. Banh, F. J. Shiou, Determination of optimal small ball-burnishing parameters for both surface roughness and superficial hardness improvement of STAVAX, Arab. J. Sci. Eng., 41 (2016) 639-652. https://doi.org/10.1007/s13369-015-1710-1

[5]. X. L. Yuan et al., Effect of roller burnishing process parameters on the surface roughness and microhardness for TA2 alloyInt, J. Adv. Manuf. Tech., 85 (2016) 1373-1383. https://doi.org/10.1007/s00170-015-8031-0

[6]. H. Amdouni, H et al., Modeling and optimization of a ball-burnished aluminum alloy flat surface with a crossed strategy based on response surface methodology, Int. J. Adv. Manuf. Tech., 88 (2017) 801-814. https://doi.org/10.1007/s00170-016-8817-8

[7]. J. Huuki, S. V. A. Laakso, Integrity of surfaces finished with ultrasonic burnishing, P. I. Mech. Eng. B-J. Eng., 227 (2012) 45-53. https://doi.org/10.1177/0954405412462805

[8]. R. Teimouri, S. Amini, A. B. Bami, Evaluation of optimized surface properties and residual stress in ultrasonic assisted ball burnishing of AA6061-T6, Measurement., 116 (2018) 129-139. https://doi.org/10.1016/j.measurement.2017.11.001

[9]. R. Teimouri, S. Amini, Analytical modeling of ultrasonic burnishing process: Evaluation of active forces, Measurement., 131 (2019) 654-663. https://doi.org/10.1016/j.measurement.2018.09.023

[10]. T. T. Nguyen, X. B. Le, Optimization of interior roller burnishing process for improving surface quality, Mater. Manuf. Process., 33 (2018) 1233-1241. https://doi.org/10.1080/10426914.2018.1453159

[11]. T. T. Nguyen, X. B. Le, Optimization of roller burnishing process using Kriging model to improve surface properties, P. I. Mech. Eng. B-J. Eng., 233 (2019) 2264-2282. https://doi.org/10.1177/0954405419835295

[12]. T. T. Nguyen et al., Multi-objective optimization of the flat burnishing process for energy efficiency and surface characteristics, Mater. Manuf. Process., 34 (2019) 1888-1901. https://doi.org/10.1080/10426914.2019.1689266

[13]. T. T. Nguyen et al., Multi-response optimization of the roller burnishing process in terms of energy consumption and product quality, J. Clean. Prod., 245 (2020) 119328 https://doi.org/10.1016/j.jclepro.2019.119328

[14]. T. T. Nguyen, V. T. Tran, M. Mia, Multi-Response Optimization of Electrical Discharge Drilling Process of SS304 for Energy Efficiency, Product Quality, and Productivity, Materials, 13 (2020), 2897. https://doi.org/10.3390/ma13132897

[15]. E. Cakit, W. Karwowski, Predicting the occurrence of adverse events using an adaptive neuro-fuzzy inference system (ANFIS) approach with the help of ANFIS input selection, Artif. Intell. Rev., 48 (2017) 139-155. https://doi.org/10.1007/s10462-016-9497-3

[16]. T. T. Nguyen, T. C.Vu, Q. D. Duong, Multi-responses optimization of finishing honing process for surface quality and production rate, J Braz. Soc. Mech. Sci. Eng., 42 (2020) 604. https://doi.org/10.1007/s40430-020-02690-y